# Image Reconstruction of a Buried Perfectly Conducting Cylinder Illuminated by Transverse Electric Waves

**Yueh-Cheng Chen, Ying-Feng Chen, Chien-Ching Chiu, Chin-Yung Chang**

Electrical Engineering Department, Tamkang University, Tamsui, Taiwan, Republic of China

*Received 9 May 2005; accepted 27 February 2006*

**ABSTRACT:** This article presents a computational approach to the image reconstruction of a perfectly conducting cylinder illuminated by transverse electric waves. A perfectly conducting cylinder of unknown shape buried in one half-space and scatters the incident wave from another half-space where the scattered field is recorded. Based on the boundary condition and the measured scattered field, a set of nonlinear integral equations is derived, and the imaging problem is reformulated into an optimization problem. The steady state genetic algorithm is then employed to find out the global extreme solution of the cost function. Numerical results demonstrated that, even when the initial guess is far away from the exact one, good reconstruction can be obtained. In such a case, the gradient-based methods often get trapped in a local extreme. In addition, the effect of different noise on the reconstruction is investigated. © 2006 Wiley Periodicals, Inc. Int J Imaging Syst Technol, 15, 261–265, 2005; Published online in Wiley InterScience (www.interscience.wiley.com). DOI 10.1002/ima.20060

**Key words:** electromagnetic imaging; transverse electric; half-space structure; perfect conductor; steady-state genetic algorithm

## I. INTRODUCTION

The inverse scattering technique for imaging the shape of a perfectly conducting cylinder has attracted considerable attention in recent years. They can apply in noninvasive measurement, medical imaging, and biological application. In the past 20 years, many rigorous methods have been developed to solve the exact equation. However, inverse problems of this type are difficult to solve, because they are ill-posed and nonlinear. As a result, many inverse problems are reformulated as optimization problems. Generally speaking, two main kinds of approaches have been developed. The first is based on gradient searching schemes such as the Newton–Kantorovitch method (Roger, 1981; Tobocman, 1989; Chiu and Kiang, 1992), the Levenberg–Marguart algorithm (Colton and Monk, 1986; Kirsch et al., 1988; Hettlich, 1994), and the successive-overrelaxation method (Kleiman and van den Berg, 1994). These methods are highly dependent on the initial guess and tend to get trapped in a local extreme. In contrast, the second approach is based on the evolutionary searching schemes (Xiao and Yabe, 1998; Chiu and Chen, 2000). They tend to converge to the global extreme of the problem, no matter what the initial estimate is (Rahmat-Samiia and Michielessen, 1999; Li et al., 2004). Owing to the difficulties in computing the Green's function by numerical method, the problem of inverse scattering in a half-space has seldom been attacked. Moreover, most microwave inverse scattering algorithms developed are for TM wave illumination in which vector problem can be simplified to a scalar one and in which less works have been reported on the more complicated transverse electric (TE) case. In the TE case, the presence of polarization charges makes the inverse problem more nonlinear. As a result, the reconstruction becomes more difficult. To the best of our knowledge, there is still no investigation for a buried conductor illuminated by TE waves. In this article, image reconstruction of a perfectly conducting cylinder buried in a half-space illuminated by TE waves is investigated. The steady state genetic algorithm (Vavak and Fogarty, 1996; Zhen et al., 2004) is used to recover the shape of the scatterer. In Section II, the theoretical formulation for the electromagnetic imaging is presented. The general principle of the genetic algorithm and the way we applied them to the imaging problem are described. Numerical results for various objects of different shapes are given in Section III. Section IV is the conclusions.

## II. THEORETICAL FORMULATION

**A. Direct Problem.** Let us consider a perfectly conducting cylinder buried in a half-space (region 2) with permittivity $\varepsilon_2$ and conductivity $\sigma_2$, above which lies another half-space (region 1) with permittivity $\varepsilon_1$ and conductivity $\sigma_1$, as shown in Figure 1. The metallic cylinder with cross section described by the equation $\rho = F(\theta)$ is illuminated by an incident plane wave, whose magnetic field vector is parallel to the $z$ axis (i.e., transverse electric or TE polarization). We assume that the time dependence of the field is harmonic with the factor $e^{j\omega t}$. Let $H_i$ denote the incident field form region 1 with incident angle $\theta_1$ as follows:

$$\vec{H}_i = e^{-jk_1(y\cos\theta_1 + x\sin\theta_1)}Z\,. \tag{1}$$

*Correspondence to:* Chien-Ching Chiu; E-mail: chiu@ee.tku.edu.tw

Owing to the interfaces, the incident plane wave generates two waves that would exist in the absence of the conducting object. Thus, the unperturbed field is given by the following equation:

$$\bar{H} = \begin{cases} (e^{-jk_1[y\cos\theta_1 + x\sin\theta_1]} + H_1 e^{-jk_1[-y\cos\theta_1 + x\sin\theta_1]})\hat{Z} & y \le -a, \\ (H_2 e^{-jk_2[y\cos\theta_2 + x\sin\theta_2]})\hat{Z} & y > -a, \end{cases} \tag{2}$$

where

$$H_1 = \left(\frac{Z_1 - Z_2}{Z_1 + Z_2}\right) e^{2jk_1 a\cos\theta_1},$$

$$H_2 = \frac{2Z_1 e^{jk_1 a\cos\theta_1} e^{-jk_2 a\cos\theta_2}}{Z_1 + Z_2}$$

$$k_1 \sin\theta_1 = k_2 \sin\theta_2$$

$$k_i^2 = \omega^2 \varepsilon_1 \mu_0 - j\omega\mu_0\sigma \qquad i = 1,2 \;\; \mathrm{Im}(k_i) \le 0,$$

$$Z_1 = \eta_1 \cos\theta_1, Z_2 = \eta_2 \cos\theta_2 \quad \eta_1 = \sqrt{\frac{\mu_1}{\varepsilon_1}} \;\; \eta_2 = \sqrt{\frac{\mu_2}{\varepsilon_2}}.$$

For TE case, the magnetic field has only one component along the $Z$ axis such that the scattered magnetic field $H_s$ at the point $(x,y)$ in Cartesian coordinates or $(r, \theta)$ in polar coordinates is given by

$$H_{\mathrm{s}}(x,y) = \int_0^{2\pi} G(x,y;F(\theta'),\theta')(j\omega\varepsilon)J_{\mathrm{sm}}(\theta')d\theta' \tag{3}$$

with

$$G(x,y;x',y') = \begin{cases} G_1(x,y;x',y') & y \le -a, \\ G_2(x,y;x',y') = G_{\mathrm{f}}(x,y;x',y') + G_{\mathrm{s}}(x,y;x',y') & y > -a, \end{cases} \tag{4}$$

where

$$G_1(x,y;x',y') = \frac{1}{2\pi}\int_{-\infty}^{\infty} \frac{j}{\gamma_1 + \gamma_2} \; e^{j\gamma_1(y+a)} \; e^{-j\gamma_2 \; (y'+a)} \; e^{-ja(x-x')} \; d\alpha, \tag{4a}$$

$$G_{\mathrm{f}}(x,y;x',y') = \frac{j}{4} H_0^{(2)}\left[k_2\sqrt{(x-x')^2 + (y-y')^2}\right] \tag{4b}$$

$$G_{\mathrm{s}}(x,y;x',y') = \frac{1}{2\pi}\int_{-\infty}^{\infty} \frac{j}{2\gamma_2}\left(\frac{\gamma_2 - \gamma_1}{\gamma_2 + \gamma_1}\right) e^{-j\gamma_2(y+2a+y')} e^{-ja(x-x')} d\alpha, \tag{4c}$$

$$\gamma_i^2 = k_i^2 - \alpha^2 \quad i = 1,2 \;\; \mathrm{IM}(\gamma_i) \le 0 \;\; y' > a.$$

Here, $J_{\mathrm{sm}}(\theta)$is the induced surface magnetic current density, which is proportional to the normal derivative of the magnetic field on the conductor surface and G($x$, $y$;$x'$, $y'$) is the Green's function which can be obtained by Fourier transform. In Eq. (4b), $H_0^{(2)}$ is the Hankel function of the second kind of order zero. We might face some difficulties in calculating the Green's function. The Green's function, given by Eq. (4), is in the form of an improper integral, which must be evaluated numerically. However, the integral converges very slowly when $r$ and $r'$ approach the interface $y = -a$. Fortunately, we find that the integral in $G_1$ or $G_{\mathrm{s}}$ may be rewritten as a closed-form term with a rapidly converging integral (Chiu and Kiang, 1990). Thus the whole integral in the Green's function can be calculated efficiently.

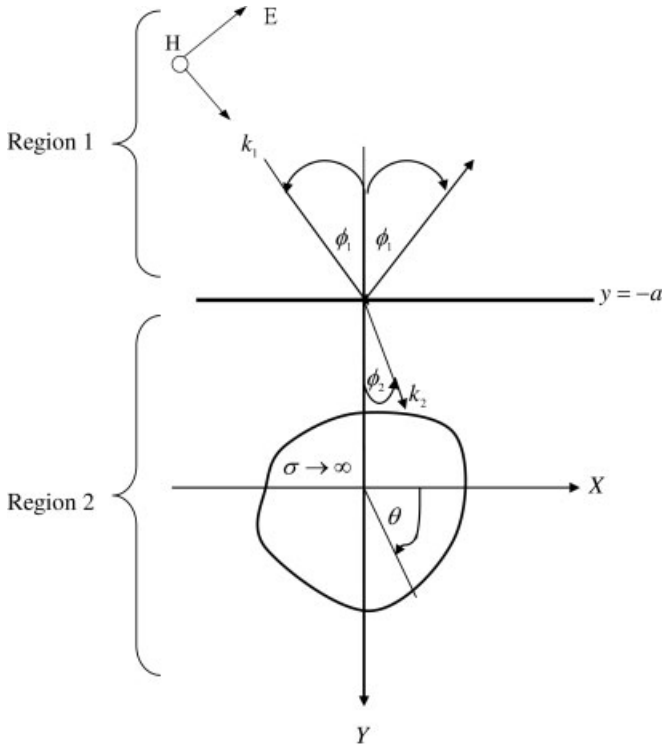


**Figure 1.** Geometry of the problem in ($x$, $y$) plane.

For a perfectly conducting scatterer, the total tangential electric field at the surface of the scatterer is equal to zero.

$$\hat{n} \times \left(\frac{1}{j\omega\varepsilon}\nabla \times H\right) = 0, \tag{5}$$

where n̂ is the outward unit vector normal to the surface of the scatterer.

For the direct scattering problem, the scattered field $H_{\mathrm{s}}$ is calculated by assuming that the shape is known. This can be achieved by first solving $J_{\mathrm{sm}}$ in Eq. (5) and then calculating $H_{\mathrm{s}}$ using Eq. (3). To verify our numerical results, the scattering field of a cylinder with circular cross section is first calculated by the analytic theorem and compared with those obtained by the moment method. It is found that a good agreement has been achieved. Moreover, the discretization number of $J_{\mathrm{sm}}(\theta)$ for the direct problem is two times than that for the inverse problem in our simulation, since it is crucial that the synthetic data generated by a direct solver are not like those obtained by the inverse solver. For the inverse problem, assume that the approximate center of scatterer, which in fact can be any point

inside the scatterer, is known. Then the shape function $F(\theta)$ can be expanded as follows:

$$F(\theta) = \sum_{n=0}^{N/2} B_n \cos(n\theta) + \sum_{n=1}^{N/2} C_n \sin(n\theta), \qquad (6)$$

where $B_n$ and $C_n$ are real coefficients to be determined, and $N + 1$ is the number of unknowns for the shape function. In the inversion procedure, the steady state genetic algorithm is used to minimize the following cost function:

$$CF = \left\{ \frac{1}{M_t} \sum_{m=1}^{M_1} \left| H_s^{\exp}(r_m) - H_N^{cal}(r_m) \right|^2 \div \left| H_s^{\exp}(r_m) \right|^2 + \alpha' (\theta) \right|^2 \Big\}^{1/2}, \qquad (7)$$

where $M_t$ is the total number of measurement points. $H_s^{\exp}(r)$ and $H_s^{\text{cal}}(r)$ are the measured and calculated scattered fields, respectively. The factor $\alpha|F'(\theta)|^2$ can be interpreted as the smoothness requirement for the boundary $F(\theta)$.

**B. Steady-State Genetic Algorithm.** The genetic algorithm is a global optimization method based on genetic recombination and evolution in nature. The iterative procedures of GA are used by starting with some randomly selected population of potential solutions, and then gradually evolve toward a better solution through the application of the genetic operators: reproduction, crossover, and mutation operators. In our problem, both parameters $B_n$ and $C_n$ are encoded using gray code. The steady-state genetic algorithm is employed for the imaging problem which has been investigated recently. The variance of the steady-state genetic algorithm is to insert the new individuals generated by crossover and mutation into the parent population to form a temporary population, and new offspring is obtained by using rank selection scheme.

It should be noted that the calculation of the Green's function is quite computational expensive. The steady-state genetic algorithm has not only the characteristic of faster convergence but also the lower rate of crossover. As a result, it is a suitable scheme to effectively save the calculation time for the inverse problem as compared with the generational GA.

## III. NUMERICAL RESULTS

We illustrate the performance of the proposed inversion algorithm and its sensitivity to random noise in the scattered field. Let us consider a perfectly conducting cylinder buried in a lossless half-space ($\sigma_1 = \sigma_2 = 0$). The permittivity in each region is characterized by $\varepsilon_1 = \varepsilon_2$ and $\varepsilon_2 = 2.55\varepsilon_1$ respectively, as shown in Figure 1. The frequency of the incident wave is chosen to be 3 GHz, i.e., the wavelength $\lambda_0$ is 0.1 m. The object is buried at a depth of $a = \lambda_0$ and the scattered field is measured on a probing line along the interface between region 1 and region 2. Our purpose is to reconstruct the shape of the object by using the scattered field at different incident angles. To reconstruct the shape of the object, the object is illuminated by incident waves from three different directions, and eight measurement points at equal spacing are used along the interface $y = -a$ for each incident angle. There are 24 measurement points in each simulation. The incident angles are equal to 45°, 90°, and 135°, respectively. The coding length of each unknown coefficient, $B_n$ (or $C_n$), is

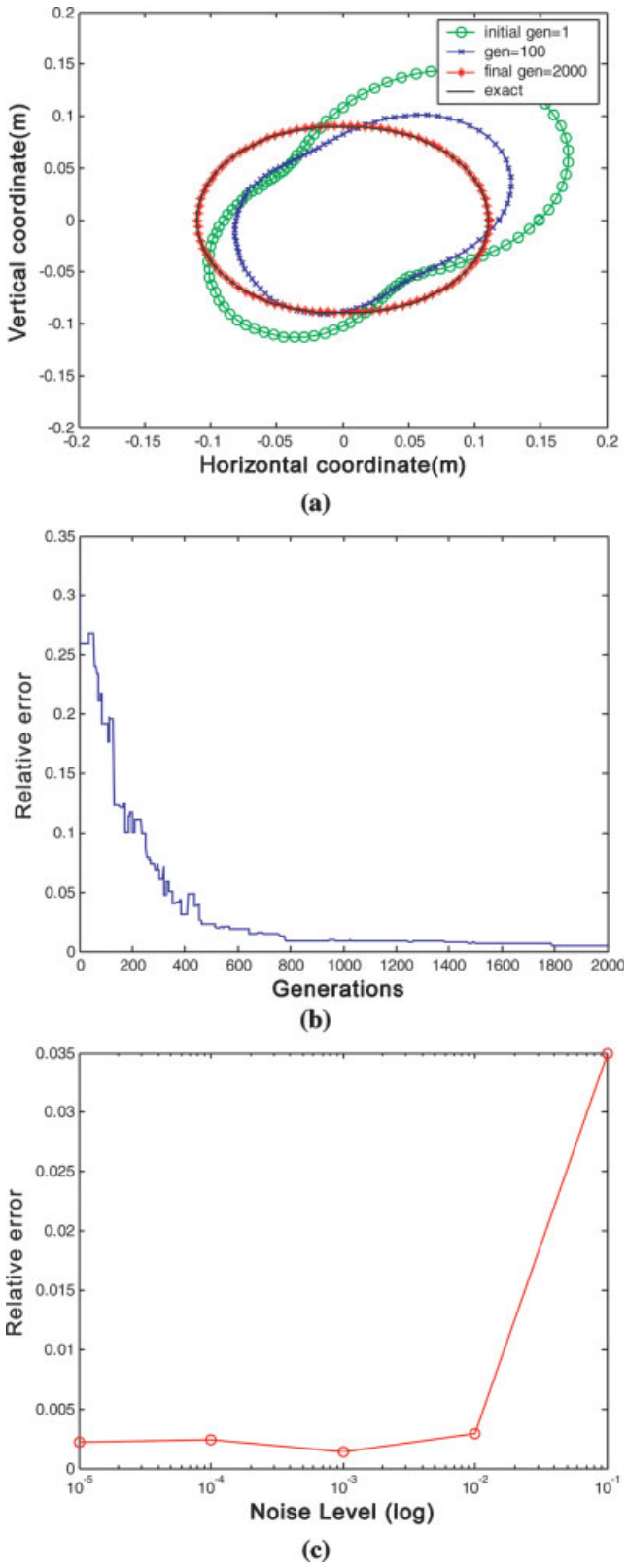


**Figure 2.** (a) Shape function for example 1. The star curve represents the exact shape, while the solid curves are calculated shape in iteration process. (b) Shape function error in each generation. (c) Shape function error as a function of noise. [Color figure can be viewed in the online issue, which is available at www.interscience.wiley.com]

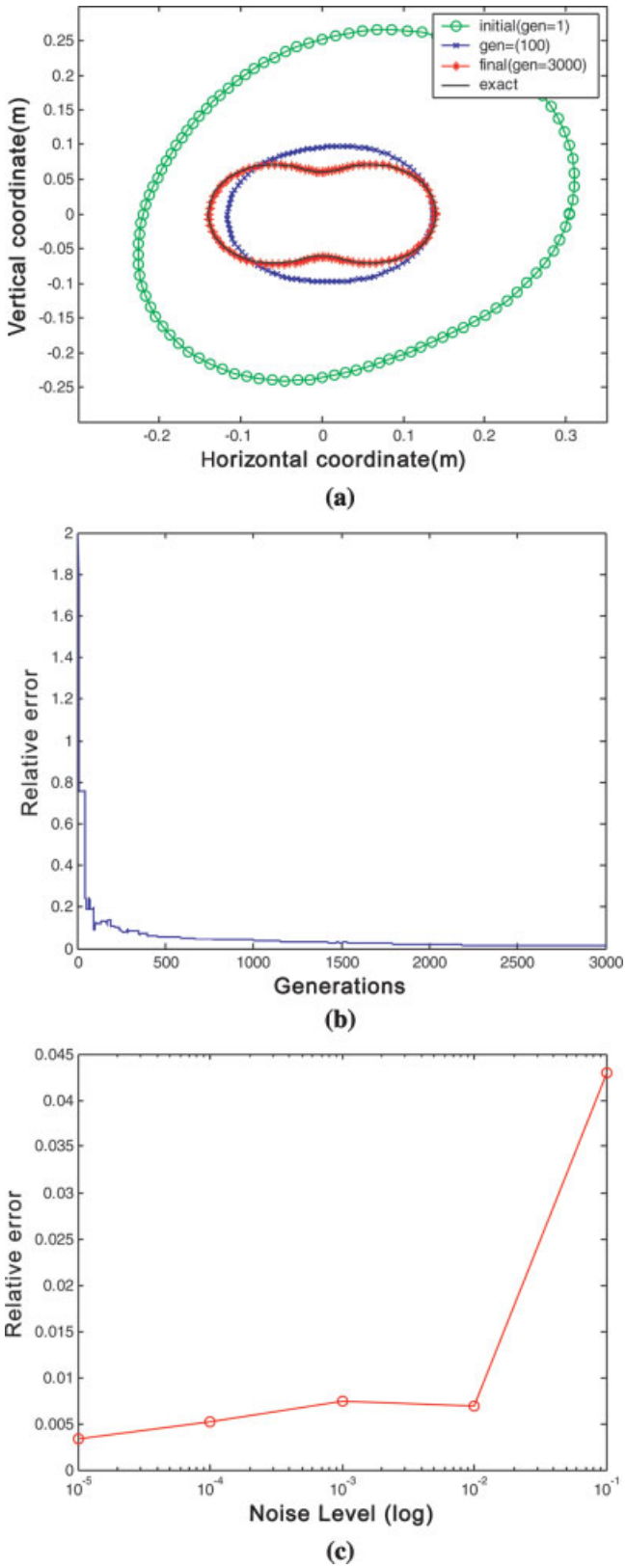


**Figure 3.** (a) Shape function for example 2. The star curve represents the exact shape, while the solid curves are calculated shape in iteration process. (b) Shape function error in each generation. (c) Shape function error as a function of noise. [Color figure can be viewed in the online issue, which is available at www.interscience.wiley.com]

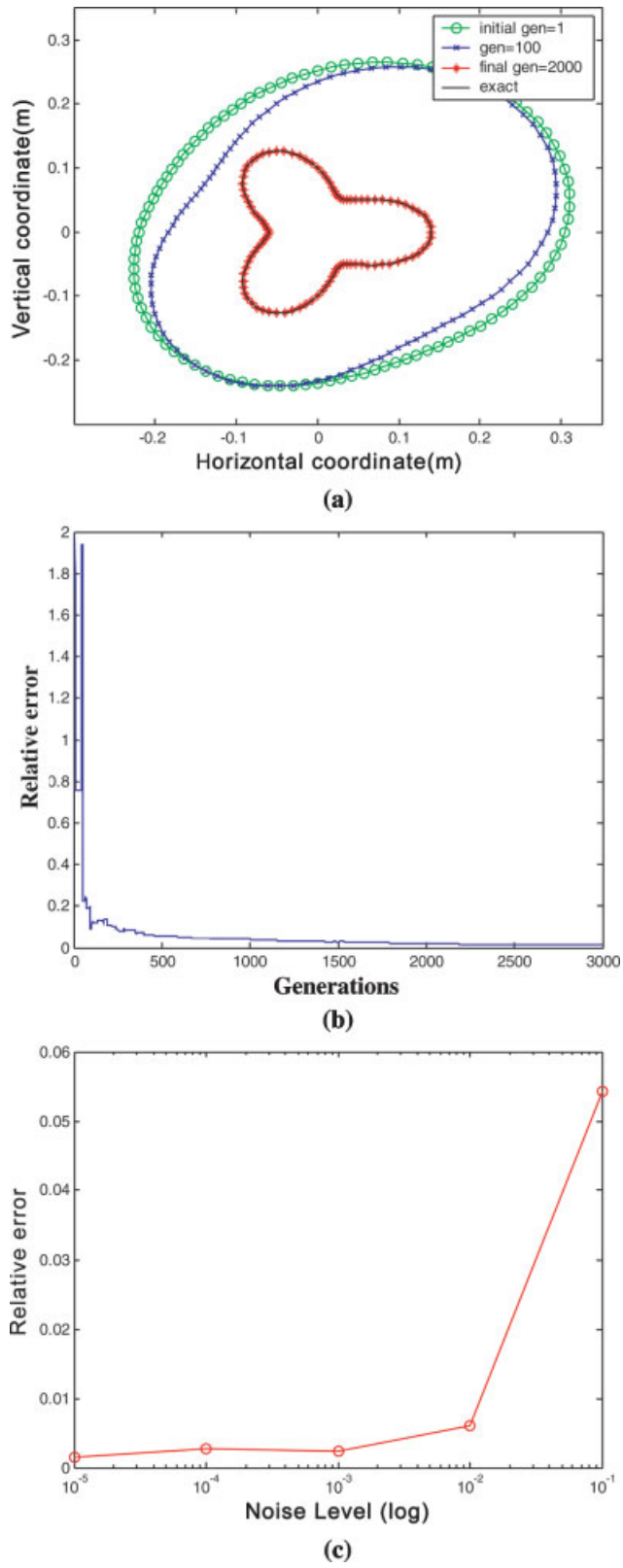


**Figure 4.** (a) Shape function for example 3. The star curve represents the exact shape, while the solid curves are calculated shape in iteration process. (b) Shape function error in each generation. (c) Shape function error as a function of noise. [Color figure can be viewed in the online issue, which is available at www.interscience.wiley.com]

set to be 16 bits. The search range for the unknown coefficient of the shape function is chosen to be from $-0.001$ to 0.05, $B_0$ is chosen to be 0.01–0.3. The crossover probability $p_c$ is equal to 0.05 and mutation probability $p_m$ is set to be 0.025. For the first example, the needed CPU time is about 2 h for the case on Celecron 2.0 GHz computer. The needed CPU time is about 3 h for the case on Celecron 2.0 GHz computer for the other examples.

In the first example, the shape function is chosen to be $F(\theta) = (0.1 + 0.01 \cos 2\theta)\ m$. The reconstructed shape function for the best population member is plotted in Figure 2a, with the shape error shown in Figure 2b. The reconstructed shape error is 2%. The CPU time for this case is about 2 h on Celecron 2.0 GHz computer.

For investigating the sensitivity of the imaging algorithm against random noise, we added the uniform noise to the real and imaginary parts of the simulated scattered fields. Normalized standard deviations of $10^{-5}$, $10^{-4}$, $10^{-3}$, $10^{-2}$, and $10^{-1}$ are used in the simulations. The shape error versus normalized noise level is plotted in Figure 2c. It is found that the effect of noise to the shape reconstruction is negligible for normalized standard deviations below $10^{-3}$. The reconstructed result is quite good.

In the second example, the shape function is chosen to be $F(\theta) = (0.1 + 0.04 \cos 2\theta)\ m$. The reconstructed shape function for the best population member is plotted in Figure 3a, with the shape error shown in Figure 3b. The reconstructed shape error is 3%. The CPU time for this case is about 3 h on Celecron 2.0 GHz computer. The shape error versus normalized noise level is plotted in Figure 3c.

In the third example, the shape function is chosen to be $F(\theta) = (0.1 + 0.04 \cos 3\theta)\ m$. The reconstructed shape function for the best population member is plotted in Figure 4a, with the shape error shown in Figure 4b. The reconstructed shape error is 3%. The CPU time for this case is about 3 h on Celecron 2.0 GHz computer. The shape error versus normalized noise level is plotted in Figure 4c.

## IV. CONCLUSIONS

We have presented a study of applying the steady-state genetic algorithm to reconstruct the shapes of an embedded conducting cylinder illuminated by TE waves through the knowledge of scattered field. Based on the boundary condition and measured scattered field, we have derived a set of nonlinear integral equations and reformulated the imaging problem into an optimization one. The genetic algorithm is then employed to de-embed the microwave image of metallic cylinder in the TE case, where the presence of polarization charges makes the inverse problem more nonlinear and more difficult. In our experience, the main difficulties in applying the genetic algorithm to the problem are to choose the suitable parameters, such as the population size, coding length of the string ($L$), crossover probability ($p_c$), and mutation probability ($p_m$). Different parameter sets will affect the speed of convergence as well as the computation time. According to our experimental result, the population size should be about 10 times of unknowns to obtain better reconstructed result. Numerical results show that good shape reconstruction can be achieved as long as the normalized noise level is $<10^{-3}$.

## REFERENCES


C.C. Chiu and W.T. Chen, Electromagnetic imaging for an imperfectly conducting cylinder by the genetic algorithm, IEEE Trans Microwave Theory Tech 48 (2000), 1901–1905.

C.C. Chiu and Y.W. Kiang, Inverse scattering of a buried conducting cylinder, Inverse Probl 7 (1990), 187–202.

C.C. Chiu and Y.W. Kiang, Microwave imaging of multiple conducting cylinders, IEEE Trans Antennas Propag 40 (1992), 933–941.

D. Colton and P. Monk, A novel method for solving the inverse scattering problem for time-harmonic acoustic waves in the resonance region II, SIAM J Appl Math 46 (1986), 506–523.

F. Hettlich, Two methods for solving an inverse conductive scattering problem, Inverse Probl 10 (1994), 375–385.

A. Kirsch, R. Kress, P. Monk, and A. Zinn, Two methods for solving the inverse acoustic scattering problem, Inverse Probl 4 (1988), 749–770.

R.E. Kleiman and P.M. van den Berg, Two-dimensional location and shape reconstruction, Radio Sci 29 (1994), 1157–1169.

C.L. Li, S.H. Chen, C.M. Yang, and C.C. Chiu, Electromagnetic imaging for a partially immersed perfectly conducting cylinder by the genetic algorithm, Radio Sci 39 (2004), RS2016.

Y. Rahmat-Samiia and E. Michielessen, Electromagnetic optimization by genetic algorithms, Wiley Interscience, New York, 1999.

A. Roger, Newton–Kantorovitch algorithm applied to an electromagnetic inverse problem, IEEE Trans Antennas Propag AP-29 (1981), 232–238.

W. Tobocman, Inverse acoustic wave scattering in two dimensions from impenetrable targets, Inverse Probl 5 (1989), 1131–1144.

F. Vavak and T.C. Fogarty, Comparison of steady state and generational genetic algorithms for use in nonstationary environments, Proc IEEE Int Conf on Evolutionary Computation, 1996, pp. 192–195.

F. Xiao and H. Yabe, Microwave imaging of perfectly conducting cylinders from real data by micro genetic algorithm coupled with deterministic method, IEICE Trans Electron E81-C (1998), 1784–1792.

S. Zhen, C. Jianlin, and Z. Huiping, Parameter design of integrated altitude control system using steady state genetic algorithm, Intelligent Control and Automation of IEEE 3 (2004) 2091–2094.